J Neurophysiol 89: 246–256, 2003;
10.1152/jn.00097.2002.

Functional Organization of Speed Tuned Neurons in Visual Area MT

JING LIU AND WILLIAM T. NEWSOME
Howard Hughes Medical Institute and Department of Neurobiology, Stanford University School of Medicine, Stanford California 94305-5125

Submitted 11 February 2002; accepted in final form 18 September 2002

Liu, Jing, and William T. Newsome. Functional organization of speed tuned neurons in visual area MT. *J Neurophysiol* 89: 246–256, 2003; 10.1152/jn.00097.2002. We analyzed the functional organization of speed tuned neurons in extrastriate visual area MT. We sought to determine whether neurons tuned for particular speeds are clustered spatially and whether such spatial clusters are elongated normal to the cortical surface so as to form speed columns. Our data showed that MT neurons are indeed clustered according to preferred speed. Multiunit recordings were speed tuned, and the speed tuning of these signals was well correlated with the speed tuning of single neurons recorded simultaneously. To determine whether speed columns exist in MT, we compared the rates at which preferred speed changed in electrode tracks that traversed MT obliquely and normally to the cortical surface. If speed columns exist, the preferred speed should change at a faster rate during oblique electrode tracks. We found, however, that preferred speed changed at similar rates for either type of penetration. In the same data set, the rate of change of preferred direction and preferred disparity differed substantially in normal and oblique penetrations as expected from the known columnar organization of MT. Thus our results suggest that a columnar organization for speed tuned neurons does not exist in MT.

INTRODUCTION

Motion is a vector defined by direction and speed. In the primate visual system, motion is represented in a specialized pathway that begins in striate cortex (V1), extends through extrastriate areas MT (V5) and MST, and terminates in higher areas of the parietal and temporal lobes. While the neural representation of direction in this pathway, and its relationship to perception, have been studied extensively, our understanding of speed representation is relatively poor. We know that most MT neurons are selective for speed (Lagae et al. 1993; Maunsell and Van Essen 1983; Perrone and Thiele 2001) and that lesions of MT and MST can impair performance on speed discrimination tasks and on eye movement tasks that require accurate computation of speed (Dursteler and Wurtz 1988; Newsome et al. 1985; Orban et al. 1995; Pasternak and Merigan 1994; Schiller and Lee 1994; Yamasaki and Wurtz 1991). Furthermore, MT in normal human subjects is more active during a speed discrimination task than during other visual discrimination tasks that do not require speed perception (Beauchamp et al. 1997; Corbetta et al. 1990 1991; Huk and Heeger 2000; but also see Sunaert et al. 2000). We do not know, however, exactly how the speed of an object is encoded within the visual cortex nor how the activity of individual neurons is related to perceptual judgments of speed.

In this study we inquire further into the neural representation of speed by examining whether speed tuned neurons in MT are organized in cortical columns. Columnar organization is a hallmark of sensory cortical organization (for a review, see Mountcastle 1997) and, where present, is strongly indicative of the central functions of a given cortical area. Thus a columnar organization for speed would suggest that speed, like direction and disparity, is a quantity of fundamental importance that is computed and represented within MT. Furthermore, a columnar organization for speed would be convenient for microstimulation experiments for testing the contribution of speed tuned neurons to visual perception as has been done successfully for motion direction (Born et al. 2000; Celebrini and Newsome 1995; Groh et al. 1998; Salzman et al. 1992; Salzman and Newsome 1994), for stereoscopic depth (DeAngelis et al. 1998), and for somatosensory frequency discrimination (Romo et al. 1998, 2000).

Local clustering of speed tuned neurons has been reported anecdotally in several studies of MT and in one study of V3 (Cheng et al. 1994; DeAngelis and Newsome 1999; Felleman and Van Essen 1987; Maunsell and Van Essen 1983), but systematic tests for columnar organization for speed have not been performed. In this study we measured speed, direction, and disparity tuning curves for single neurons and multineuron clusters at regular intervals along electrode penetrations traversing MT. We compared the rate of change of preferred speed, direction, and disparity in penetrations that traversed MT approximately normal and oblique to the cortical surface. If MT contains a columnar organization for speed, preferred speed should change rapidly from site to site for oblique penetrations and slowly if at all for normal penetrations. Our measurements confirmed the previously demonstrated columnar organization for direction and binocular disparity (Albright et al. 1984; DeAngelis and Newsome 1999). Speed tuning properties, however, changed at similar rates in both normal and oblique penetrations. We conclude that little or no columnar organization for speed exists in MT.

METHODS

Monkey maintenance and surgery

We conducted extracellular recordings in three hemispheres of two macaque monkeys (*Macacca mulatta*), one male and one female.

Address for reprint requests: J. Liu, Department of Neurobiology, Stanford University School of Medicine, Fairchild Building, Room D209, Stanford, CA 94305 (E-mail: jingliu@stanford.edu).

The costs of publication of this article were defrayed in part by the payment of page charges. The article must therefore be hereby marked "*advertisement*" in accordance with 18 U.S.C. Section 1734 solely to indicate this fact.

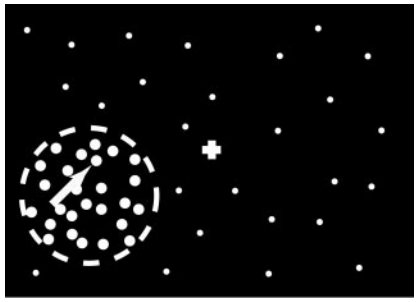

FIG. 1. Schematic illustration of the visual display. The monkey viewed a moving random dot stimulus peripherally while maintaining fixation on the cross. Arrow indicates the direction of motion of the dots in the receptive field (dashed circle). The background of the screen was filled with small, flickering dots at zero disparity to assist the monkey in maintaining accurate vergence on the fixation cross. See METHODS for details. Dashed circle represents the receptive field of the MT site at the electrode tip; it is for illustration purposes only and was not present in the actual experiments.

Prior to the experiments, the monkeys were surgically implanted with a head-holding device and recording cylinder (Crist Instruments) and a scleral search coil for monitoring eye position. All implanted devices were MRI compatible. Surgical, animal care, and experimental procedures conformed to guidelines established by the National Institutes of Health.

Visual stimuli and behavioral task

During each experimental session, the monkey was seated in a primate chair with its head fixed. The monkey viewed visual stimuli on a CRT monitor at a distance of 57 cm. Visual stimuli were drawn with a VSG graphics board (Cambridge Research Systems, Kent, England); the refresh rate of the monitor was 160 Hz. The monkey viewed the display through computer-controlled ferroelectric liquid crystal shutters (DisplayTech) so that we could control the disparity of the visual stimuli. The left and right eye shutters opened alternately and were synchronized with the refresh rate of the monitor.

At the beginning of each trial, a small, white fixation cross ($0.35 \times 0.35°$) appeared on a dark background. After the monkey fixated the cross, moving random dots appeared inside a circular aperture for 1 s (Fig. 1). In each trial, all dots moved in the same direction, with the same speed and binocular disparity; any of these three parameters could be varied randomly from trial to trial to measure the appropriate tuning curve. To maintain a constant dot density, each dot that left the aperture reentered from the other side at a random location. The size of each dot was $0.23 \times 0.23°$, and the dot density was usually 32 dots/s/deg^2. With a lifetime of 18.75 ms for each dot, the dot density of the stimulus at a given moment in time was 0.6 dots/deg^2.

Eye movements were measured throughout each experiment using the scleral search coil technique. The monkey was required to maintain fixation within a $2 \times 2°$ window centered on the fixation cross. The background of the screen was filled with flickering dots having the same disparity (zero) as the fixation cross. Using search coils in each eye to monitor vergence angle, DeAngelis and Newsome (1999) showed that this background facilitates accurate fixation and vergence in the presence of stimuli with disparity. The background dots were small ($0.12 \times 0.12°$) and were presented at a density of 4 dots/deg^2/s. With a lifetime of 18.75 ms for each dot, the density of the background dots at any given moment of time was 0.075 dots/deg^2. Trials in which the monkey broke fixation before the end of the stimulus presentation were deemed error trials and discarded. The monkey received a liquid reward after each successful trial.

Moving dots were drawn with subpixel precision (Georgeson et al. 1996), enabling us to present smoothly moving stimuli at speeds as low as 0.3 deg/s. We limited speeds to 76.8 deg/s or below, since the perception of smooth motion deteriorated noticeably at higher speeds due to the limited refresh rate of the monitor.

Recording cylinder locations and data collection

We employed tungsten microelectrodes with impedences of approximately 1 MΩ (FHC), introduced to the cortex through a transdural guide tube positioned within a plastic grid inside the recording cylinder. To access MT, we placed two recording cylinders on each monkey, one permitting microelectrodes to traverse MT approximately normal to the cortical surface (Fig. 2*A*) and the other permitting oblique traverses across MT (Fig. 2*B*). In monkey C, the anterior cylinder permitted access to MT in the left hemisphere while the posterior cylinder permitted access to the right hemisphere. In monkey W, both cylinders were positioned on the right hemisphere, allowing us to compare the rate of change in preferred speed for oblique and near-normal penetrations in the same MT. Oblique penetrations crossed V1 and the lunate sulcus before reaching MT. Near-normal penetrations crossed the central sulcus, the intraparietal sulcus, and the anterior bank of the superior temporal sulcus before reaching MT. As illustrated in Fig. 2, we verified the cylinder locations and electrode trajectories in monkey C by imaging the brain with a 1.5-T MR scanner. We used a fast spin echo pulse sequence with inversion recovery preparation [repetition time (TR) = 5500 ms, echo time (TE) = 15 ms, inversion time (TI) = 350 ms, single echo, the receiver bandwidth = 32 kHz]. Contiguous, 3-mm-thick parasagittal slices were obtained along the long axis of each cylinder. We visualized the recording cylinders and the plastic grid by filling the cylinders and the grids with saline, which appears bright white in the MR images in Fig. 2. We then extrapolated a straight line from the guide tube holes in the grid to MT in the superior temporal sulcus (thin white lines in Fig. 2). This analysis confirmed that our oblique penetrations traversed MT at an angle of roughly 10° with respect to the cortical surface, while near-normal penetrations traversed MT at an angle of roughly 80°.

The depth of the electrode in the brain was controlled by a hydraulic microdrive (Narishige Scientific Instrument Lab, Tokyo, Japan). Neural voltage signals were amplified, filtered (Bak Electronics), and displayed on an oscilloscope. Because our primary goal was to assess the columnar structure of MT, the bulk of our recordings were of multiunit activity (MU), which allowed us to sample the combined activity of several neurons near the electrode tip. In these recordings, a "neural event" was considered to be any deflection of the voltage trace above an arbitrarily determined amplitude threshold within a fixed time window. This threshold was set manually so that the spontaneous activity in the absence of a visual stimulus was between 50 to 100 events/s at all recording sites. Single-unit (SU) activity was

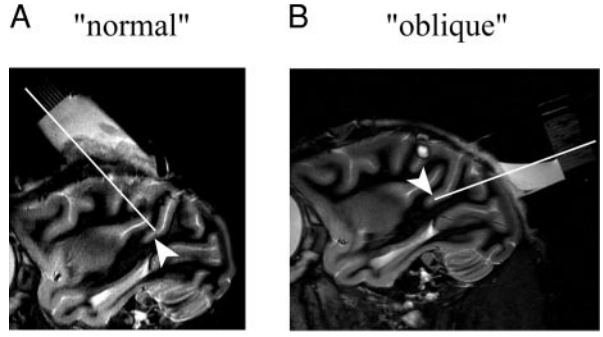

FIG. 2. MRI images of cylinder locations relative to MT in monkey C. The slices are in a parasagittal plane. The arrows indicate the location of MT in the superior temporal sulcus. The recording cylinders, partially filled with saline (bright white), are visible above the brain. Electrodes reached MT through a plastic grid fitted on top of the cylinder; grid holes are faintly visible as the thin lines above each cylinder. The long, thin white lines represent typical electrode trajectories through the grid and into the superior temporal sulcus. *A*: electrode penetrations from the anterior cylinder entered MT at an angle of roughly 80° with respect to the plane of the cortical surface (arrowhead). *B*: penetrations from the posterior cylinder entered MT at an angle of roughly 10° with respect to the surface (arrowhead).

recorded simultaneously with MU activity whenever possible using a second window discriminator.

Tuning curves were measured at regular intervals (100 or 150 μm) along each penetration. At each recording site, we used an interactive stimulus presentation program to assess qualitatively the location and size of the receptive field (RF) and the preferred direction, speed, and binocular disparity of neurons at the recording site. The center of the random dot stimulus then was positioned on the center of the RF, and the size of the stimulus was adjusted to match the size of the RF. We then quantitatively measured the tuning properties at each recording site. To measure speed tuning, we recorded responses to 10 speeds ranging from 0.3 to 76.8 deg/s (9 of the speeds were evenly spaced on a log scale, and the 10th was 60 deg/s), while setting the direction and disparity of the dots at the preferred values for the site. In a separate block, we assessed direction tuning by measuring responses to eight directions at 45° intervals, while setting the speed and the disparity of the dots at the preferred values. At some sites, disparity tuning was also measured in a third block, with the speed and direction set at the preferred values. The range of disparities employed was usually −1.2 to 1.2°, at intervals of 0.3°. For sites that preferred very "far" or very "near" disparities, the range was shifted so that the preferred value was always included in the measurement. Within each block, trials were pseudorandomly interleaved, and each condition was repeated five times.

Data analysis

We considered the response to a visual stimulus to be the average firing rate during the 1-s stimulus presentation. When we recorded MU and SU activity simultaneously, we deleted any "event" in the MU data that occurred within ±1 ms of an SU spike. This ensured independence of the MU and SU measurements (see RESULTS).

To analyze speed tuning properties, we first determined whether a site was tuned for stimulus speed using a one-way ANOVA (with speed as the main factor) and a criterion of $P = 0.01$. For each speed tuned site, we fitted the speed responses with a smoothing cubic spline function (Fig. 3*A*) (Shikin and Plis 1995). The knots of the spline were the 10 speeds for which we measured neural responses. We set the smoothness of the spline so that, for the majority of the sites, the speed tuning properties derived from the fitted curves agreed well with our visual inspection of the raw data. The same degree of smoothness was applied to fitted data from all sites. We considered the "preferred" speed to be the speed that corresponded to the peak of the fitted spline. A speed tuning index (STI) was calculated for each site according to the formula

$$STI = \frac{R_{max} - R_{min}}{R_{max} - R_{spont}} \quad (1)$$

where R_{max} is the peak response on the speed tuning curve, R_{min} is the lowest response, and R_{spont} is the spontaneous activity. This index can vary from minus infinity to plus infinity. Positive *STI* values indicate that the preferred visual stimulus was excitatory, generating an R_{max} higher than the spontaneous activity level. Negative values occurred rarely, indicating sites for which all visual stimuli were inhibitory. An index of 0 indicates no tuning. For positive *STI*s, larger values represent increasingly stronger speed tuning. An index > 1 indicates that the site was excited by its preferred speed but suppressed by some nonpreferred speeds.

We considered a site to be band-pass if the response fell below 90% of the peak response on both sides of the fitted tuning curve. The width of the tuning curve was defined as the full width of the curve at 90% of the best response ($R_{max} - R_{spont}$). Each site (or SU) in our data set was categorized into one of five classes according to their speed tuning properties. *1*) *Band-pass* (Fig. 4*A*, *E*, and *F*) and *2*) *band-rejected* (Fig. 4*B*); these sites yielded strong responses for low and high speeds, but lower responses for intermediate speeds. Thus the tuning curves showed a clear trough at intermediate speeds. *3*) *High-pass* (Fig. 4*C*), at these sites, the response to the highest speed exceeded 90% of $R_{max} - R_{spont}$; *4*) *low-pass* (Fig. 4*D*), at these sites, the response to the lowest speed exceeded 90% of $R_{max} - R_{spont}$; and *5*) *not tuned*, these sites were not speed tuned according to the ANOVA test ($P \geq 0.01$).

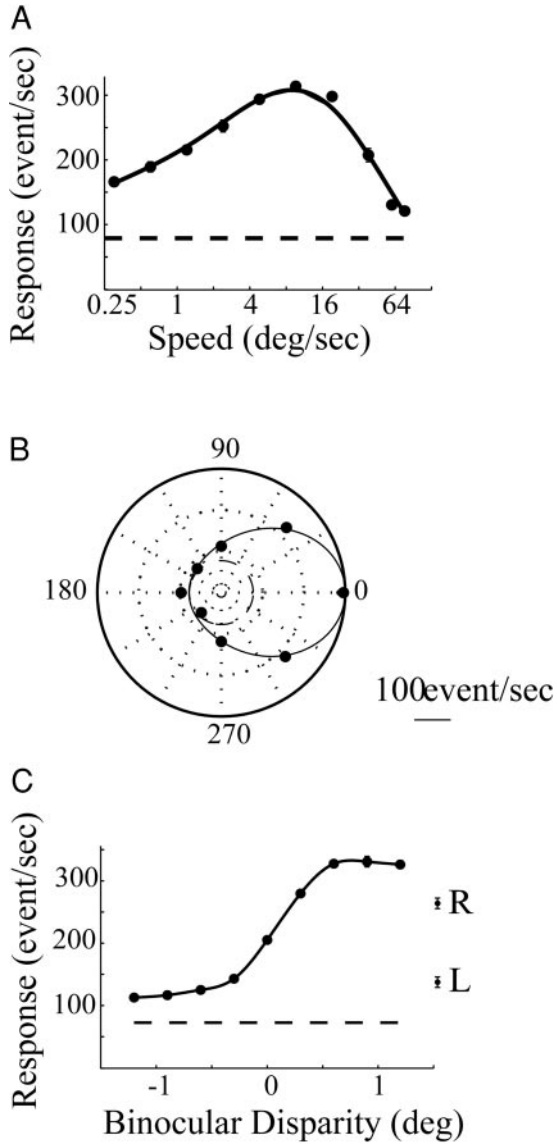

FIG. 3. Multiunit (MU) responses from a typical MT recording site. Data points indicate the mean firing rate for each stimulus condition along with the SE. (SEs are often smaller than the size of the data points). Dashed horizontal lines indicate the spontaneous activity. *A*: speed tuning curve. Data were fitted with a smoothing cubic spline. Preferred speed of this site was 9 deg/s, the tuning width was 2.19 octave, and the speed tuning index was 0.84. *B*: direction tuning curve. Data were fitted with a von Mises curve. Preferred direction of this site was 0°, with a tuning width of 110°, and a direction tuning index of 1.0. *C*: binocular disparity tuning curve. Data were fitted with an interpolating cubic spline. Data points adjacent to L and R are monocular responses from the left and the right eyes, respectively. This site preferred far disparities; the optimal disparity was 0.76°, and the tuning index was 0.85.

A cutoff level of 90% of the maximum response in the categorization process might appear, at first glance, to be overly generous. The responses we measured, however, were generally quite reliable; the standard error bars at individual speeds were usually much <10% of the total excursion in response across the tuning curve (see examples in Fig. 4). Using a cutoff value of 80%, for example, would eliminate

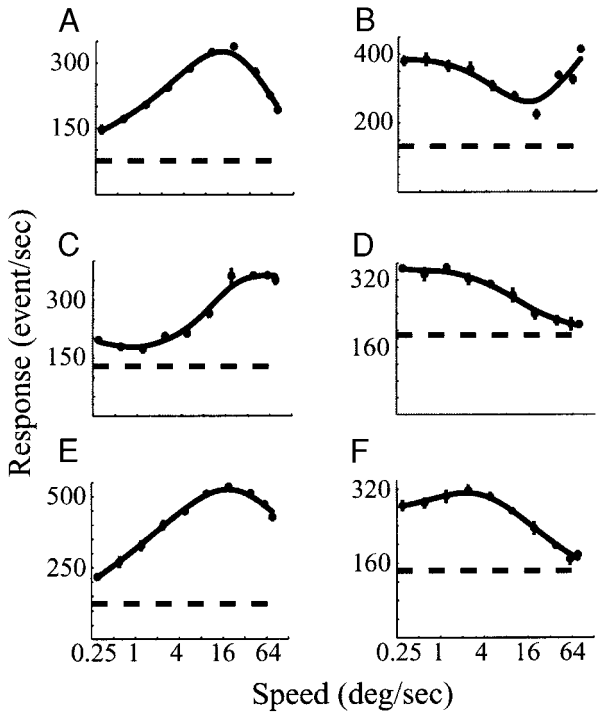

FIG. 4. Classification of speed tuning curves. *A*: a band-pass site. Preferred speed of this site was 13.4 deg/s, with a tuning width of 2.25 octaves and a tuning index of 0.73. *B*: a site that is "band-rejected." *C*: high-pass site. *D*: low-pass site. *E*: band-pass site with a preferred speed of 22.8 deg/s, a tuning width of 2.4 octaves, and a tuning index of 0.82. This site would have been classified as high-pass if we had used a cutoff criterion of 80% (or lower) of the maximum response. *F*: band-pass site with a preferred speed of 2.2 deg/s, a tuning width of 4.32 octaves, and a tuning index of 0.67. This site would have been classified as low-pass if we had used a cutoff value of 80% (or lower) of the maximum response. See METHODS for details of classification.

the curves in Fig. 4, *E* and *F*, from the band-pass category, which seems inappropriate from visual inspection of the data. We selected the 90% value because it was the most appropriate as judged by visual inspection of the entire data set. Using cutoff values of 80 or 70% reduced the number of band-pass sites in the data set and increased tuning widths but did not otherwise affect the results presented in this paper. The speed tuning properties of our sample are similar to those reported in previous studies if we adopt the criteria employed in those studies: using 50% maximum response as the cutoff value, we found that 44% of SUs in our sample were band-pass with average bandwidth of 3.64 octave (Cheng et al. 1994; Lagae et al. 1993; Maunsell and Van Essen 1983).

To identify direction tuned sites, we employed a one-way ANOVA (with direction as the main factor) and a criterion of $P \leq 0.01$. For direction tuned sites, we fitted the direction responses with a von Mises curve (Fig. 3*B*), which is the circular approximation of a Gaussian distribution (Mardia 1972)

$$\boldsymbol{y} = \boldsymbol{a} + \boldsymbol{b} \times \boldsymbol{e}^{\boldsymbol{c} \times \cos(\boldsymbol{x} - \boldsymbol{d})} \quad (2)$$

Here, the firing rate, **y**, is a function of stimulus direction, **x**, where **a** is the baseline firing rate, **b** is the amplitude, **c** is the width of tuning, and **d** is the preferred direction of the fitted function. Analyses described later in the paper (for example, Fig. 12) depend critically on the estimates of the preferred direction obtained from the fitted curves. To ensure that our fits were reasonable, we calculated an *F* ratio to determine whether the von Mises curve described the data better than a circle; we excluded from further analysis any site with an *F* ratio smaller than 2.36 (Draper and Smith 1981). This criterion rejected the poorly fitted sites (including bidirectional sites) as judged by eye. We considered the preferred direction of the site to be the direction that corresponded to the peak response and the tuning width to be the full width of the curve at 50% of the maximum response ($R_{max} - R_{spont}$). A direction tuning index was calculated similarly to the speed tuning index.

As with speed and direction, we determined whether a site was disparity selective using a one-way ANOVA and a criterion of $P \leq 0.01$. We fitted the disparity tuning curve with an interpolating cubic spline, with knots at each disparity for which responses were measured (Fig. 3*C*) (Shikin and Plis 1995). We considered the preferred disparity to be the disparity that elicited the peak response, and we computed a disparity tuning index analogous to the one described above for speed.

RESULTS

We recorded MU responses at 736 sites in two monkeys (C and W): 374 sites in 29 oblique penetrations and 362 sites in 30 near-normal penetrations. We recorded speed and direction tuning curves at almost every site. Disparity tuning curves were obtained at a subset of sites (305 sites in 23 oblique penetrations and 178 in 15 near-normal penetrations). We also recorded the local field potential (LFP) at 84 sites (low cutoff frequency, 10 Hz; high cutoff frequency, 150 Hz; sampling frequency, 1 kHz.). The preferred directions, speeds, and disparities computed from the LFP data agreed well with those computed from MU responses (data not shown). We used MU responses for most analyses in this paper, but the results would have been the same had we used LFPs. Most MU sites in our sample were tuned for direction (82.3%), speed (92.2%), and disparity (67%), as illustrated by the typical tuning curves depicted in Fig. 3.

We categorized MU sites into five speed tuning classes as described under METHODS. Of 732 sites for which we obtained speed data, 464 sites (63.4%) were band-pass (Fig. 4, *A*, *E*, and *F*); 154 (21%) were high-pass (Fig. 4*C*); 55 (7.5%) were low-pass (Fig. 4*D*); 2 (0.3%) were band-rejected (Fig. 4*B*); and 57 (7.8%) were not tuned. The number of band-pass sites we report is presumably an underestimate because the refresh rate of the monitor limited us to speeds of 76.8 deg/s or slower (see METHODS). In previous studies that used moving bars at higher speeds, a small proportion of MT neurons had preferred speeds in the range of 80–256 deg/s (e.g., Cheng et al. 1994; Lagae et al. 1993; Maunsell and Van Essen 1983).

We also recorded SU responses to speed at 55 sites in the two monkeys. Of these, 63% were band-pass; 9% were low-pass, and 15% were high-pass. Direction tuning responses were recorded for 46 SU; 78% were direction tuned. Disparity tuning responses were recorded for 35 single units; 74% showed disparity tuning.

Clustering of speed tuned cells in MT

Two of our observations indicate that speed tuned neurons are spatially clustered in MT, meaning that speed tuning properties are similar for neurons in close proximity to each other. First, a large majority of the MUs in our sample were speed tuned (92.2%) with clearly unimodal tuning curves. If neurons with different speed tuning properties were randomly interspersed within MT, MU tuning curves should be substantially less well tuned than SU tuning curves. This is not the case. Second, preferred speeds of band-pass sites were well correlated for simultaneously recorded MU and SU responses ($r = 0.77$, $P < 10^{-4}$;

Fig. 5), indicating that a SU was generally representative of the MU cluster in the immediate vicinity. (Recall that we deleted the SU signals from the MU data, ensuring that the correlation cannot be an artifact caused by one SU contributing to both SU and MU signals—see METHODS.) Comparison of SU and MU data yielded similar correlation coefficients for direction and disparity selectivity (preferred direction, $r = 0.90$, $P < 10^{-4}$; preferred disparity, $r = 0.76$, $P < 10^{-3}$), consistent with the known spatial clustering of direction and disparity tuned neurons in MT (Albright et al. 1984; DeAngelis and Newsome 1999). The computed coefficient for the preferred speeds presumably underestimates the actual correlation because the analysis was based only on band-pass sites; we also observed that the SU tuning curve predicted the occurrence of low- or high-pass responses in the simultaneously measured MU response (data not shown).

The similarities in speed tuning of nearby neurons might simply be a secondary result of a correlation between preferred speed and other variables that vary systematically across MT such as retinal eccentricity and RF size. Preferred speed is known to be correlated modestly with eccentricity (Cheng et al., 1994; Maunsell and Van Essen 1983; but also see Lagae et al. 1993). RF size also is correlated with retinal eccentricity (Albright and Desimone 1987; Maunsell and Van Essen 1987), raising the possibility that preferred speed may be correlated with RF size. In principle, then, the correlation in Fig. 5 could reflect the fact that the MU and SU pairs share similar RF size and eccentricity. Over the restricted range of eccentricities that we recorded, however, we failed to find a correlation between the RF eccentricity and preferred speed in either our MU or SU sample. We did observe a very weak but significant correlation between preferred speed and RF size in our MU sample ($r = 0.12$, $P < 0.01$), but this weak relationship cannot contribute substantially to the observed correlation between MU and SU preferred speed.[1]

For sites at which both the SU and MU responses were band-pass, tuning widths were not correlated, although tuning widths of the MU curves tended to be larger than those of the SU curves (MU: 2.30 ± 0.65 octave; SU: 1.99 ± 0.57 octave; *t*-test, $P < 10^{-4}$). The speed tuning indices of MUs and SUs were not correlated, and there was no significant tendency for the MU indices to be smaller than those of SUs. All of these data are consistent with the notion that a band-pass MU is composed of several SUs, all band-pass and having similar but not identical preferred speeds.

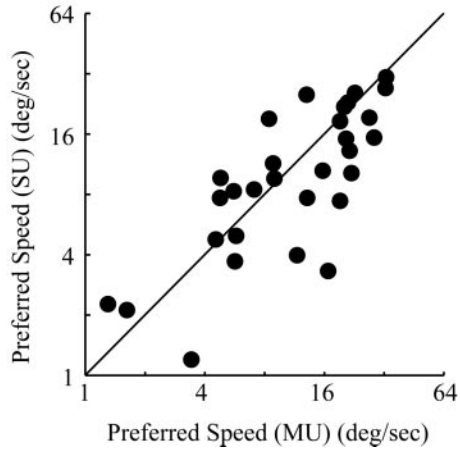

FIG. 5. Scatter plot of preferred speeds for simultaneously recorded MU and single unit (SU) responses. The straight line is the equality line. The correlation coefficient is 0.77 ($P < 10^{-4}$, $n = 30$).

Comparison of oblique and near-normal penetrations

To determine whether speed tuned neurons in MT form cortical columns, we compared the rate of change of preferred speed as our microelectrode traversed MT in oblique versus near-normal penetrations. The irregular morphology of the superior temporal sulcus precluded precisely tangential or normal penetrations, but our analysis only requires a substantial difference in angle between the oblique and near-normal penetrations. As described under METHODS, MRI images indicate that the penetrations in monkey C were within 10–15° of their intended trajectories (Fig. 2). If speed tuned neurons are organized into cortical columns, the rate of change of preferred speed with penetration distance should be substantially more rapid in oblique as compared with near-normal penetrations. Knowing that MT has a columnar organization for direction and disparity, we measured direction and disparity tuning properties as a positive control for our evaluation of columnar architecture.

Figure 6 shows the speed tuning curves at each of 13 sites in a representative oblique penetration. Tuning curves were collected every 0.15 mm in this penetration. The preferred speed fluctuated irregularly at the first three sites, but then progressed smoothly from 7.9 to 31 deg/s at sites 4 through 12, an increase of 3.9-fold. The preferred speed then dropped back to 7.5 deg/s at the final site, 13. Figure 7*A* summarizes the change in preferred speeds along this penetration, and Fig. 7*B* depicts the change in preferred direction. As was the case for preferred speed, the preferred direction varied systematically along the length of the penetration, except in a small region of nondirectional sites encountered in the first third of the penetration. RF position also changed during the course of the penetration (Fig. 7*C*) from an initial position near the horizontal meridian at an eccentricity of 4.3° to a slightly more eccentric location higher in the upper quadrant.

Figure 8 summarizes results from another oblique penetration. In this penetration, the preferred speeds were low for the first two sites and then shifted abruptly to higher speeds and became high-pass in the middle of the penetration. In the

[1] We conducted a partial correlation analysis to evaluate the possible contribution of RF size to the correlation between MU and SU preferred speed. The appropriate partial correlation formula is

$$R_{ms} = \frac{r_{ms} - r_{mr} \times r_{sr}}{\sqrt{(1 - r_{mr}^2)(1 - r_{sr}^2)}} \quad (3)$$

where R_{ms} is the corrected correlation that we wish to calculate, and r_{ms}, r_{mr}, and r_{sr} are the observed correlations between preferred speeds of MUs and SUs (r_{ms}), between preferred speeds of MUs and RF size (r_{mr}), and between the preferred speeds of SUs and RF size (r_{sr}) (Zar 1998). Unfortunately, we do not know the value of r_{sr} because the receptive field size of the single units was not measured in the experiments (the aperture sizes were always determined by the size of the multiunit receptive field). We can, however, place bounds on the possible values of R_{ms} by differentiating *Eq. 3* after substituting in the values of r_{ms} and r_{mr} that we did measure. Differentiation shows that the relationship defined by *Eq. 3* has a single minimum at a value of 0.768 for R_{ms}, which does not differ appreciably from the originally measured value of 0.77. Such a small effect of the RF size is not surprising given the weak correlation between RF size and preferred speeds of MUs. Thus the observed correlation between the preferred speeds of MU and SU recordings (Fig. 5) is not driven artifactually by RF size.

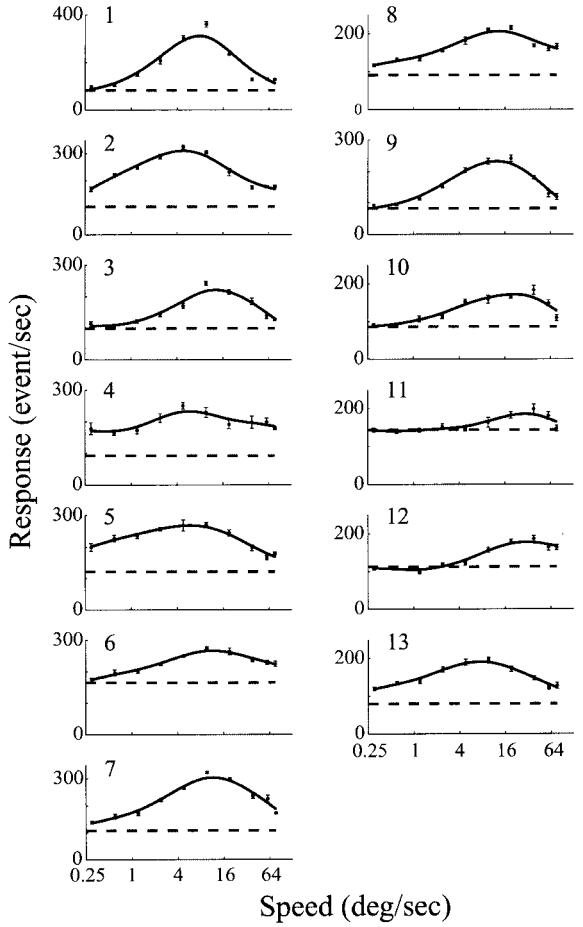

FIG. 6. Speed tuning curves for each of the 13 sites in a representative oblique penetration. MU responses to speeds were recorded every 150 μm. The mean responses are plotted together with the SE; the dashed lines indicate the spontaneous activity level.

second half of the penetration, the sites became band-pass once again, varying smoothly among speeds $>$ 16 deg/s for several hundred microns before becoming high-pass again at the end of the penetration. As illustrated in Fig. 8*B*, preferred direction also changed smoothly in this penetration. The first half of the penetration was particularly striking, with preferred direction progressing from 75 to 214° and then back to 35°. Several nontuned sites were then encountered, followed by more direction tuned sites at the end of the penetration. RFs (Fig. 8*C*) were in the lower quadrant, but moved closer to the horizontal meridian during the penetration.

Figure 9 shows speed tuning curves at each of the 11 sites, sampled at 0.1-mm intervals, in a representative near-normal penetration. In this penetration, the preferred speed changed from 2 to 19 deg/s, an increase of 9.5-fold. From site 3 to site 11, the shifts in preferred speed were nicely monotonic. Figure 10 summarizes the data from this penetration. In contrast to the speed tuning data (Fig. 10*A*), the preferred direction changed little over the course of the penetration (only 50°, Fig. 10*B*). Consistent with the near-normal electrode trajectory, RF centers were tightly clustered in the upper quadrant just above the horizontal meridian (Fig. 10*C*).

Figure 11 depicts similar data from another near-normal penetration. The preferred speed increased from 1 to 6.25 deg/s and then decreased to 2.45 deg/s before becoming low-pass at the end of the penetration (Fig. 11*A*). The preferred direction changed gradually over about 80° in the first millimeter of the penetration (Fig. 11*B*). While this rate of change in preferred direction was faster than in the experiment of Fig. 10, it was considerably more modest than in the oblique penetrations illustrated in Figs. 7 and 8. The last site in Fig. 11 preferred a direction of 24°, a change of 137° from the site nearest it. This type of discontinuity—a sudden change of about 180°—occurs occasionally in MT (Albright et al. 1984; DeAngelis and Newsome 1999). RF centers changed modestly in the upper quadrant during the penetration (Fig. 11*C*).

Qualitatively, Figs. 6–11 reveal little if any difference in the rate of change of preferred speed in oblique and near-normal penetrations. In contrast, the same penetrations show substantial differences in the rate of change of preferred direction and

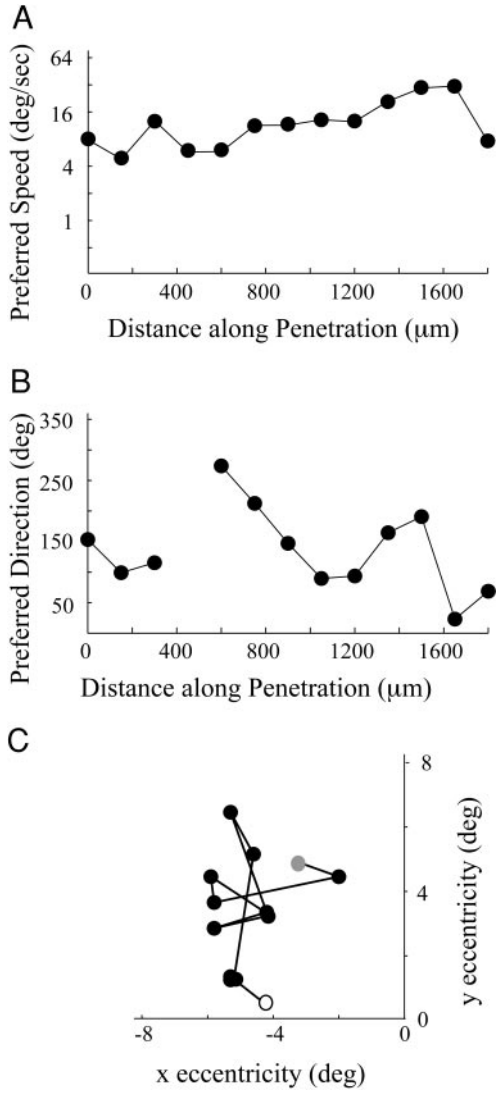

FIG. 7. Summary of the data for the oblique penetration illustrated in Fig. 6. MU tuning curves for speed and direction were recorded every 150 μm. *A*: preferred speed at each recording site plotted against the distance along the electrode penetration in MT. *B*: preferred direction at each recording site plotted against the distance along the electrode penetration. Blank locations indicate nondirectional sites. *C*: locations of the receptive fields (RFs) for all the sites in this penetration. Each circle represents the center of one RF. The RF locations of the first and the last sites are indicated by the open circle and the gray circle, respectively. The fixation point was at (0,0).

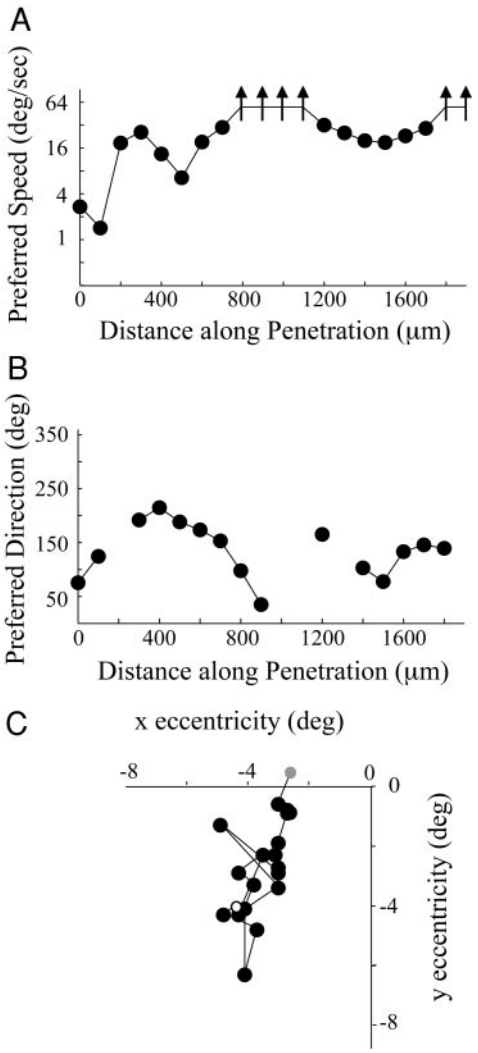

FIG. 8. Summary of the data for another oblique penetration. MU tuning curves for speed and direction were recorded every 100 μm. The format of this figure is identical to that shown in Fig. 7. Upward arrows in *A* indicate high-pass sites.

receptive field location, consistent with the known columnar structure and retinotopic layout of MT (Albright and Desimone 1987; Maunsell and Van Essen 1987; Van Essen et al. 1981).

Quantitative analysis

To confirm the above observations quantitatively, we first compared the preferred speed of each site in a particular penetration with the preferred speed of every other site in the same penetration. If both sites in a paired comparison were band-pass, we calculated the ratio of their preferred speeds and indexed that ratio by the distance in microns between the two recording sites. We then pooled the data from all oblique or near-normal penetrations, obtaining the geometric mean of ratios of preferred speeds for sites separated by 100, 200, 300 μm, and so on. The estimates of the mean ratio are less reliable for large separations because fewer pairs of points are available for comparison in each penetration. The columnar organization hypothesis predicts that this ratio will increase faster for oblique compared with near-normal penetrations. [We employed ratios to describe the difference in speed tuning between sites because perceptually discriminable speed differences follow Weber's Law (for example, see Fig. 1 in De Bruyn and Orban 1988), suggesting that neural representation of speeds is logarithmic. In fact, most speed tuning curves would be strongly skewed toward higher speeds if plotted on linear scale (see Fig. 4*A* for an example)].

Figure 12*A* shows the result of this analysis. The mean ratio of preferred speeds is plotted as a function of the distance between the pairs of recording sites. The ratio increased almost linearly as a function of distance between sites for both types of penetrations. This observation confirms once again that speed tuned neurons are clustered in MT since preferred speeds were more similar (ratios closer to unity) for adjacent sites than for widely separated sites. The horizontal dashed line shows the mean ratio of preferred speed obtained from pairs of sites selected randomly with no regard for intersite distance. The horizontal line thus provides an indication of the value of the ratio if speed tuned neurons are randomly organized in MT. The observed values approach the "random" value for intersite distances of 500–600 μm, suggesting that the spatial scale of organization of speed tuned neurons is on the order of half a millimeter.

Importantly, the curves for near-normal and oblique penetrations are quite similar for the first 600–700 μm of separation. To compare the curves statistically, we performed a two-way ANOVA, using the ratio as the dependent variable,

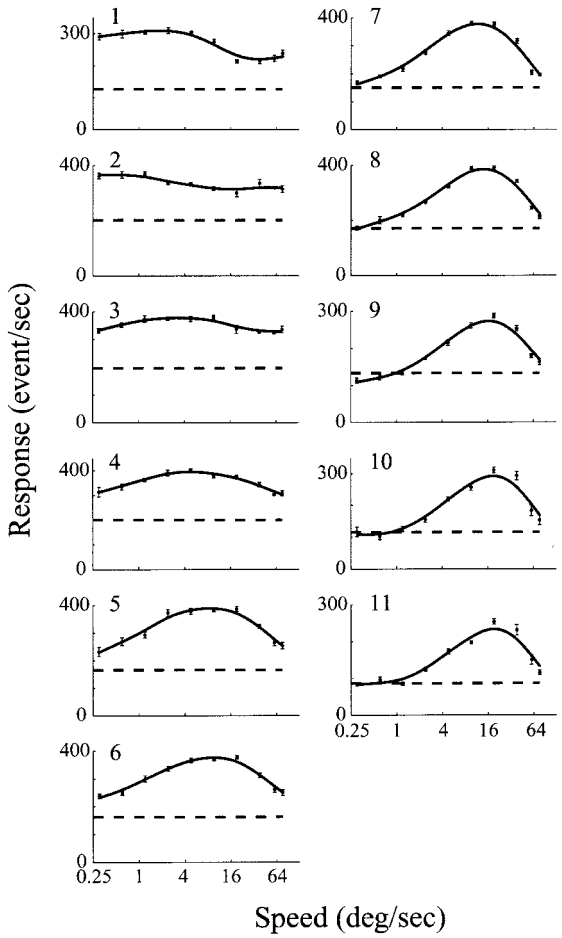

FIG. 9. Speed tuning curves for each of the 11 sites in a representative near-normal penetration. MU responses to speeds were recorded every 100 μm. The format is identical to that shown in Fig. 6.

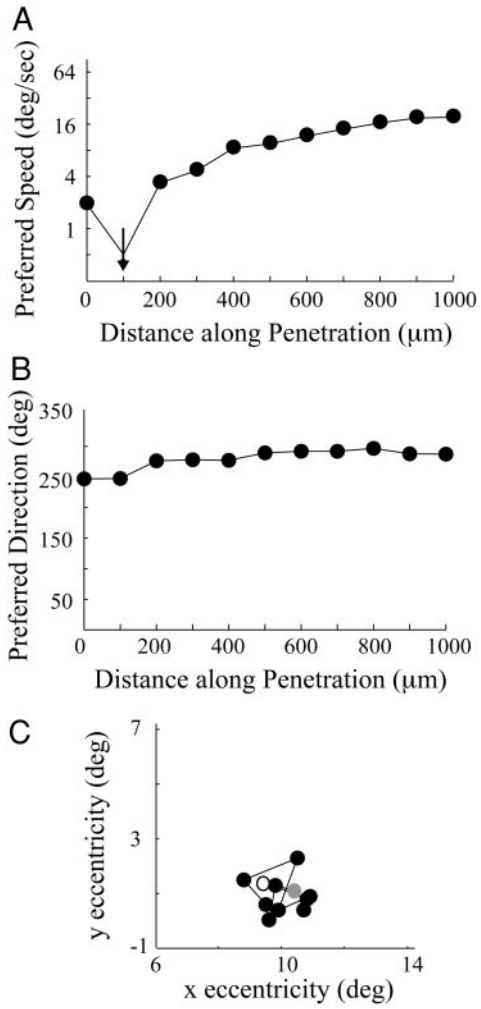

FIG. 10. Summary of the data for the near-normal penetration illustrated in Fig. 9. The format of this figure is identical to that shown in Fig. 7. Downward arrows in *A* indicate low-pass sites. The fixation point was at (0,0) but is not shown in *C*. The eccentricity scale on each axis is equal to the scales in Figs. 7*C* and 8*C* so that the reader can easily compare the amount of RF scatter in these penetrations.

and the distance between sites and the penetration type as independent variables. The analysis revealed a significant effect of interpair distance as expected [$F(9,2017) = 36.31$, $P < 0.001$] and penetration type as well [$F(1,2017) = 9.42$, $P < 0.01$]. The former effect was mostly driven by data points in the first 600–700 μm of separation, whereas the latter effect was mostly driven by the few, less reliable data points for large separations (fewer pairs were available for large separations). When we repeated the two-way ANOVA on data points with 600 μm or less separation, the effect of interpair distance was still significant [$F(5,1591) = 35.82$, $P < 10^{-6}$], but the penetration type had no significant effect [$F(1,1591) = 1.88$, $P = 0.17$]. Repeating the two-way ANOVA on data points separated by more than 600 μm revealed a significant effect of penetration type [$F(1,426) = 15.1$, $P = 10^{-4}$], but not interpair distance [$F(3,426) = 1.03$, $P = 0.38$]. We also repeated the two-way ANOVA with the RF size as a covariate to rule out the possibility that the differences in the preferred speeds were caused solely by the RF size. The results were very similar to those obtained when no covariate was used.

The above analysis was performed on combined data from two monkeys. When we analyzed separately the data from each monkey, the results were essentially the same. Note that the placement of recording cylinders in monkey W allowed us to sample from the same MT in both oblique and near-normal angles (see METHODS), further confirming that the lack of speed columns is genuine.

It is possible that our failure to demonstrate columnar organization for speed is attributable to an insufficient difference in the penetration angles for near-normal and oblique penetrations. Figure 12, *B* and *C*, however, show that this is not the case. The figures depict the difference in preferred direction and disparity as a function of distance for the same penetrations. The difference in preferred direction increases as a function of intersite distance for both oblique and near-normal penetrations, but the rate of increase is much higher in oblique penetrations, consistent with previous findings (Albright et al. 1984; DeAngelis and Newsome 1999). A two-way ANOVA showed a significant effect of intersite distance [$F(9,3139) =$

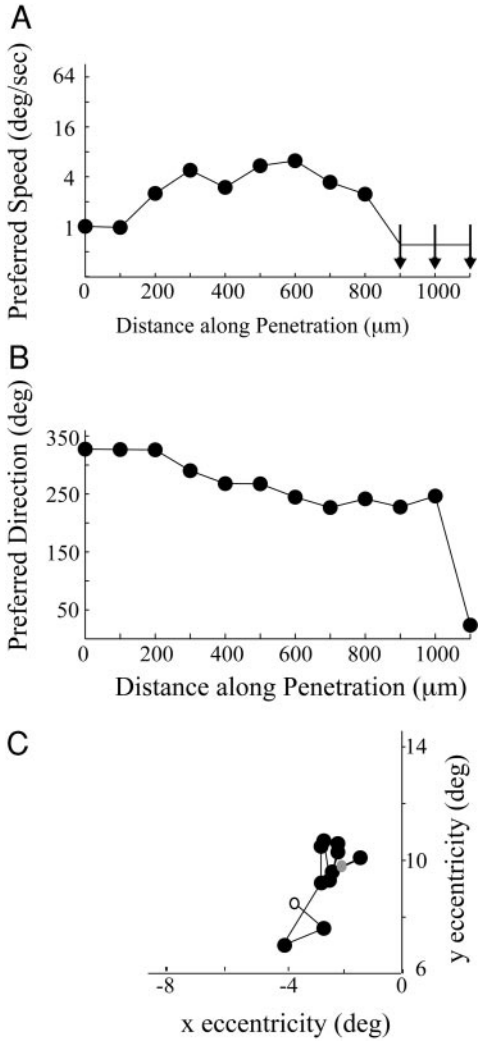

FIG. 11. Summary of the data for another near-normal penetration. MU responses to speeds and directions were recorded every 100 μm. The format is identical to that shown in Fig. 7. Downward arrows in *A* indicate low-pass sites. The fixation point was at (0,0) but is not shown in *C*. eccentricity scale on each axis is equal to the scales in Figs. 7*C* and 8*C* so that the reader can easily compare the amount of RF scatter in these penetrations.

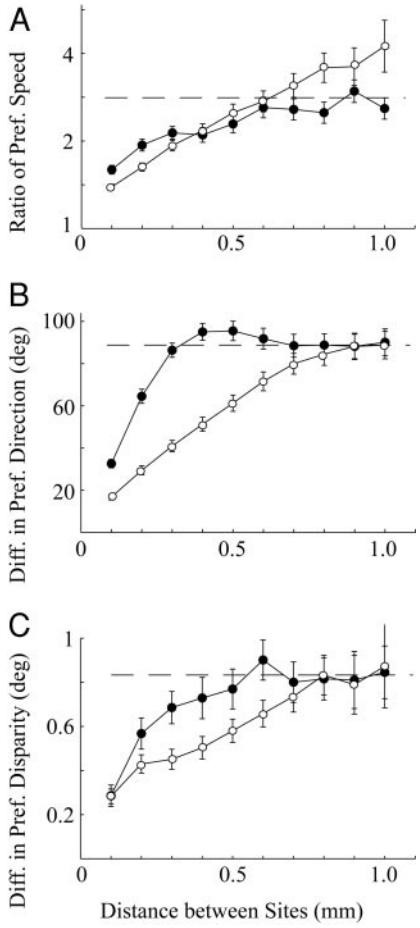

FIG. 12. Quantitative summary of the comparison between oblique and near-normal penetrations. Filled circles and the open circles are data from oblique and near-normal penetrations, respectively. *A*: mean ratio of preferred speeds between pairs of sites plotted as a function of the distance between sites in the pair. The ratio is always more than 1 because we always calculated the ratio of the faster speed to the slower speed. Each data point is plotted together with the SE. Dashed line represents the expected value when pairs of MT sites are arbitrarily selected and their preferred speeds are compared. *B*: similar plot for the average absolute difference in preferred directions. *C*: similar plot for the average absolute difference in preferred disparities in monkey C.

68.84, $P < 10^{-4}$] and penetration type [$F(1,3139) = 63.29$, $P < 10^{-4}$] on the change in preferred direction. Furthermore, regression analysis revealed that the slope of the initial phase of the curve for oblique penetrations (the first 0.4 mm) is significantly steeper than that for the near-normal penetrations (the first 1 mm; $P < 10^{-3}$).

Our sample of disparity tuned sites, while smaller than the samples of speed and direction tuned sites, produced similar results (Fig. 12*C*). A two-way ANOVA revealed significant effects of intersite distance [$F(9,691) = 7.55$, $P < 10^{-4}$] and penetration type [$F(1,691) = 4.54$, $P = 0.033$] on preferred disparity. Again, a regression analysis confirmed this result; the slope of the first 0.6 mm for the oblique curve was significantly steeper than that of the first 0.6 mm for the near-normal curve ($P < 0.01$).

Given the sharp contrast between the organization of speed tuned cells and the organizations of direction and disparity tuned cells, we conclude that columnar structure for speed was either absent or very weak in these two monkeys, despite the obvious spatial clustering of speed tuned neurons.

Other analyses

We examined our data set for possible relationships between preferred speed and preferred disparity across the population of recording sites. Because the speed of a moving object on the retina is inversely proportional to the distance of the object from an observer, we wondered whether preferred speed might be systematically related to disparity, with sites preferring near disparities also preferring faster speeds. We also entertained the hypothesis that higher preferred speeds might be related to larger preferred disparities of either sign (near or far) since parallax-induced motion of an object on the retina increases in speed as the distance of the object from the horopter increases. Our sample of speed and disparity tuned sites, however, did not reveal either of these relationships. We observed a positive correlation between preferred speed and preferred disparity (of either sign) in one monkey ($r = 0.44$, $P < 0.01$), but found a weak negative correlation in the other monkey ($r = -0.16$, $P = 0.02$). When we analyzed separately sites that preferred far and near disparities, we found no consistent relationship.

DISCUSSION

The primary goals of this study were to determine whether speed tuned neurons in MT are spatially clustered and, if so, whether the clusters are elongated perpendicularly to the cortical surface so as to form columns. Our data indicate that speed tuned neurons are indeed clustered, but do not form cortical columns, at least not in the two monkeys in our study. Three observations indicate that speed tuned neurons in MT are spatially clustered: *1*) most MU sites were speed tuned with well behaved, unimodal tuning curves; *2*) preferred speeds of SUs and MUs recorded simultaneously were well correlated (Fig. 5); and *3*) the difference in preferred speed for pairs of MU recording sites increased monotonically with the distance between the recording sites (Fig. 12*A*). Importantly, however, the rate of change of preferred speed with penetration distance was very similar for near-normal and oblique penetrations (Fig. 12*A*), indicating that any columnar organization for speed was weak if not completely absent. Direction tuning and disparity tuning data obtained on the same penetrations confirmed the known columnar organization for these parameters (Albright et al. 1984; DeAngelis and Newsome 1999). Thus our failure to find evidence for speed columns cannot be attributed to poor differentiation between oblique and near-normal penetrations.

It is conceivable that speed tuned neurons could be organized in "minicolumns," at a finer spatial scale than is easily detected with the sampling frequency of our recordings (every 100–150 μm). In this scheme, each direction or "axis-of-motion" column would contain a representation of the full range of possible speeds. We are skeptical of this possibility for two reasons. First, we were indeed able to detect regularities in the organization of speed tuned neurons using our sampling strategy. The summary data in Fig. 12 show clearly that the preferred speeds at adjacent recording sites are far more similar than would be expected by chance. Furthermore, the spatial scale of the organization is roughly similar to the scale of organization of direction columns tangential to the cortical surface (400–500 μm). If our sampling intervals were too coarse to detect spatial regularities in the distribution of preferred speeds, the summary curves in Fig. 12 should be

essentially flat at the level expected by chance. Second, there is little or no hint of fine spatial organization in our comparison of SU and MU data recorded simultaneously. If preferred speed were organized in minicolumns at a spatial scale finer than 100–150 μm (our sampling intervals), one would expect multiunit speed tuning curves to exhibit substantially less selectivity than those of single units. This was not the case, however, as indicated under RESULTS. Tuning widths of MU curves were 2.30 octaves on average ($\pm$0.65 octave), only modestly broader than those of SU recorded simultaneously (1.99 $\pm$ 0.57 octaves). Despite this evidence, it remains possible that we could have missed subtle, fine-scale organization of speed tuned neurons.

We were somewhat surprised by the apparent lack of columnar organization for speed. MT is known to play a prominent role in motion processing within the primate visual system, and speed is one of the two defining parameters of vector motion, the other being direction. Some psychophysical evidence suggests, however, that the neural computation of speed is more complex than the computation of direction. For example, the perception of speed can depend substantially on the contrast, color, and spatial frequency composition of a stimulus (for examples, see Dougherty et al. 1999; Stone and Thompson 1992; Thompson 1982; but also see McKee et al. 1986), whereas the perception of direction appears to be substantially independent of these factors. Speed perception is also modified by the distance of an object from the subject—an effect known as speed constancy—again suggesting that the computation of speed is contextual and, by inference, less rigidly linked to elementary patterns of activity within the cortical circuitry (for example, see Zohary and Sittig 1993). Given the complexity of speed perception, it is possible that columnar organization does not provide an efficient means for performing the underlying computations.

What role, then, do speed-tuned MT neurons play in the perception of speed? No compelling answer to this question exists as yet. On the one hand, lesion studies indicate that MT contributes to the psychophysical perception of speed and to the computation of speed for the guidance of pursuit and saccadic eye movements (Dursteler and Wurtz 1988; Newsome et al. 1985; Orban et al. 1995; Pasternak and Merigan 1994; Schiller and Lee 1994; Yamasaki and Wurtz 1991). Recent physiological evidence also suggests that some MT neurons, unlike V1 neurons, combine spatial and temporally tuned inputs so as to compute speed independently of the spatial and temporal structure of the stimulus (Perrone and Thiele 2001). This observation, if confirmed, would provide strong evidence that speed information relevant to behavioral use is processed in MT. In addition, human imaging studies have shown that MT is more activated when subjects perform tasks that require the assessment of stimulus speed (Beauchamp et al. 1997; Corbetta et al. 1990, 1991; Huk and Heeger 2000; but also see Sunaert et al. 2000). On the other hand, Groh and colleagues (Groh et al. 1998; Born et al. 2000) employed electrical microstimulation to introduce a motion vector into MT during a pursuit initiation task but found that the stimulation effects were not consistently related to the speed tuning properties recorded at the stimulation site.

New studies will be necessary to resolve this issue. The spatial clustering of MT neurons that we have demonstrated raises the possibility that electrical microstimulation could be employed to examine the role of MT neurons in speed perception. To date microstimulation of sensory cortex has biased perceptual decisions only for stimulus parameters that are organized in columns (Born et al. 2000; DeAngelis et al. 1998; Groh et al. 1998; Romo et al. 1998, 2000; Salzman et al. 1992; Salzman and Newsome 1994), but, to our knowledge, experiments have not been attempted for stimulus parameters organized at smaller spatial scales. Another potential source of insight is to determine whether speed selective MT neurons exhibit significant "choice probabilities" in the context of a threshold speed discrimination task (Britten et al. 1996; Celebrini 1994; Dodd et al. 2001). If fluctuations in the firing intensity of MT neurons correlate with the psychophysical decisions made by the monkey on a trial-to-trial basis, the case for a central role for MT in speed perception would be strengthened considerably. Both of these experiments will be attempted in our laboratory in the near future.

REFERENCES

Albright TD and Desimone R. Local precision of visuotopic organization in the middle temporal area (MT) of the macaque. *Exp Brain Res* 65: 582–592, 1987.

Albright TD, Desimone R, and Gross CG. Columnar organization of directionally selective cells in visual area MT of the macaque. *J Neurophysiol* 51: 16–31, 1984.

Beauchamp MS, Cox RW, and DeYoe EA. Graded effects of spatial and featural attention on human area MT and associated motion processing areas. *J Neurophysiol* 78: 516–520, 1997.

Born RT, Groh JM, Zhao R, and Lukasewycz SJ. Segregation of object and background motion in visual area MT: effects of microstimulation on eye movements. *Neuron* 26: 725–734, 2000.

Britten KH, Newsome WT, Shadlen MN, Celebrini S, and Movshon JA. A relationship between behavioral choice and the visual responses of neurons in macaque MT. *Visual Neurosci* 13: 87–100, 1996.

Celebrini S and Newsome WT. Neuronal and psychophysical sensitivity to motion signals in extrastriate area MST of the macaque monkey. *J Neurosci* 14: 4109–4124, 1994.

Celebrini S and Newsome WT. Microstimulation of extrastriate area MST influences performance on a direction discrimination task. *J Neurophysiol* 73: 437–448, 1995.

Cheng K, Hasegawa T, Saleem KS, and Tanaka K. Comparison of neuronal selectivity for stimulus speed, length, and contrast in the prestriate visual cotical areas V4 and MT of the macaque monkey. *J Neurophysiol* 71: 2269–2280, 1994.

Corbetta M, Miezin FM, Dobmeyer S, Shulman GL, and Peterson SE. Attentional modulation of neural processing of shape, color, and velocity in humans. *Science* 248: 1556–1559, 1990.

Corbetta M, Miezin FM, Dobmeyer S, Shulman GL, and Peterson SE. Selective and divided attention during visual discriminations of shape, color, and speed: functional anatomy by positron emission tomography. *J Neurosci* 11: 2383–2402, 1991.

DeAngelis GC, Cumming BG, and Newsome WT. Cortical area MT and the perception of stereoscopic depth. *Nature* 394: 677–680, 1998.

DeAngelis GC and Newsome WT. Organization of disparity-selective neurons in macaque area MT. *J Neurosci* 19: 1398–1415, 1999.

De Bruyn B and Orban GA. Human velocity and direction discrimination measured with random dot patterns. *Vision Res* 28: 1323–1335, 1988.

Dodd JV, Krug K, Cumming BG, and Parker AJ. Perceptually bistable three-dimensional figures evoke high choice probabilities in cortical area MT. *J Neurosci* 21: 4809–4821, 2001.

Dougherty RF, Press WA, and Wandell BA. Perceived speed of colored stimuli. *Neuron* 24: 893–899, 1999.

Draper NR and Smith H. *Applied Regression Analysis* (2nd ed.). NewYork: Wiley, 1981.

Dursteler MR and Wurtz RH. Pursuit and optokinetic deficits following chemical lesions of cortical areas MT and MST. *J Neurophysiol* 60: 940–965, 1988.

Felleman DJ and Van Essen DC. Receptive field properties of neurons in area V3 of macaque monkey extrastriate cortex. *J Neurophysiol* 57: 889–920, 1987.

Georgeson MA, Freeman TCA, and Scott-Samuel NE. Sub-pixel accuracy: psychophysical validation of an algorithm for fine positioning and movement of dots on visual displays. *Vision Res* 36: 605–612, 1996.

Groh JM, Born RT, and Newsome WT. How is a sensory map read out? Effects of microstimulation in visual area MT on saccades and smooth pursuit eye movements. *J Neurosci* 17: 4312–4330, 1998.

Huk AC and Heeger DJ. Task-related modulation of visual cortex. *J Neurophysiol* 83: 3525–3536, 2000.

Lagae L, Raiguel S, and Orban GA. Speed and direction selectivity of macaque middle temporal neurons. *J Neurophysiol* 69: 19–39, 1993.

Mardia KV. *Statistics of Directional Data.* London: Academy Press, 1972.

Maunsell JHR and Van Essen DC. Functional properties of neurons in middle temporal visual area of the macaque monkey. I. Selectivity for stimulus direction, speed and orientation. *J Neurophysiol* 49: 1127–1147, 1983.

Maunsell JHR and Van Essen DC. Topographic organization of the middle temporal visual area in the macaque monkey: representational biases and the relationship to callosal connections and myeloarchitectonic boundaries. *J Comp Neurol* 266: 535–555, 1987.

McKee SP, Silverman GH, and Nakayama K. Precise velocity discrimination despite random variations in temporal frequency and contrast. *Vision Res* 26: 609–619, 1986.

Mountcastle VB. The columnar organization of the neocortex. *Brain* 120: 701–722, 1997.

Newsome WT, Wurtz RH, Dursteler MR, and Mikami A. Deficits in visual motion processing following ibotenic acid lesions of the middle temporal visual area of the macaque monkey. *J Neurosci* 5: 825–840, 1985.

Orban GA, Saunders RC, and Vandenbussche E. Lesions of the superior temporal cortical motion areas impair speed discrimination in the macaque monkey. *Eur J Neurosci* 7: 2261–2276, 1995.

Pasternak T and Merigan WH. Motion perception following lesions of the superior temporal sulcus in the monkey. *Cereb Cortex* 4: 247–259, 1994.

Perrone JA and Thiele A. Speed skills: measuring the visual speed analyzing properties of primate MT neurons. *Nat Neurosci* 4: 526–532, 2001.

Romo R, Hernandez A, Zainos A, Brody CD, and Lemus L. Sensing without touching: psychophysical performance based on cortical microstimulation. *Neuron* 26: 273–278, 2000.

Romo R, Hernandez A, Zainos A, and Salinas E. Somatosensory discrimination based on cortical microstimulation. *Nature* 392: 387–390, 1998.

Salzman CD, Murasugi CM, Britten KH, and Newsome WT. Microstimulation in visual area MT: effects on direction discrimination performance. *J Neurosci* 12: 2331–2355, 1992.

Salzman CD and Newsome WT. Neural mechanisms for forming a perceptual decision. *Science* 264: 231–237, 1994.

Schiller PH and Lee K. The effects of lateral geniculate nucleus, area V4, and middle temporal (MT) lesions on visually guided eye movements. *Vis Neurosci* 11: 229–241, 1994.

Shikin EV and Plis AI. *Handbook on Splines for the User*. Boca Raton, FL: CRC, 1995.

Stone LS and Thompson P. Human speed perception is contrast dependent. *Vision Res* 32: 1535–1549, 1992.

Sunaert S, Van Hecke P, Marchal G, and Orban GA. Attention to speed of motion, speed discrimination, and task difficulty: an fMRI study. *NeuroImage* 11: 612–623, 2000.

Thompson P. Perceived rate of movement depends on contrast. *Vision Res* 22: 377–390, 1982.

Van Essen DC, Maunsell JHR, and Bixby JL. The middle temporal visual area in the macaque: myeloarchitecture, connections, functional properties and topographic organization. *J Comp Neurol* 199: 293–326, 1981.

Yamasaki DS and Wurtz RH. Recovery of function after lesions in the superior temporal sulcus in the monkey. *J Neurophysiol* 66: 651–673, 1991.

Zohary E and Sittig AC. Mechanisms of velocity constancy. *Vision Res* 33: 2467–2478, 1993.